

SIMULATION STUDIES OF GAS-SOLID IN THE RISER OF A CIRCULATING FLUIDIZED BED

Ahmad Hussain^{1,*}, Farid Nasir Ani¹, Amer Nordin Darus¹, Azeman Mustafa², Arshad A. Salema²

¹**Faculty of Mechanical Engineering, Universiti Teknologi Malaysia, Skudai 81310, Johor, Malaysia**

²**Faculty of Chemical and Natural Resources Engineering, Universiti Teknologi Malaysia, Skudai 81310, Johor, Malaysia**

***Corresponding Author: Phone: +607-5534785, Fax: +607-5566159**

***Email: ahmad@siswa.utm.my**

ABSTRACT

A numerical parametric study was performed on the influence of various riser exit geometries on the hydrodynamics of gas-solid two-phase flow in the riser of a Circulating Fluidized Bed (CFB). A Eulerian continuum formulation was applied to both phases. A two fluid framework has been used to simulate fully developed gas-solid flows in vertical riser. A two dimensional Computational Fluid Dynamics (CFD) model of gas-particle flow in the CFB has been investigated using the code FLUENT. The turbulence was modeled by a k- ϵ turbulence model in the gas phase. The simulations were done using the geometrical configuration of a CFB test rig at the Universiti Teknologi Malaysia (UTM). The CFB riser column has 265 mm (width), 72 mm (depth) and 2.7 m height. The riser is made up of interchangeable Plexiglas columns. The computational model was used to simulate the riser over a wide range of operating and design parameters. In addition, several numerical experiments were carried out to understand the influence of riser end effects, particle size, gas solid velocity and solid volume fraction on the simulated flow characteristics. The CFD model with a k- ϵ turbulence model for the gas phase and a fixed particle viscosity in the solids phase showed good mixing behaviour. These results were found to be useful in further development of modeling of gas solid flow in the riser.

Keywords: CFD, Eulerian, hydrodynamics, riser, turbulence model.

INTRODUCTION

Despite the widespread applications of the CFB, much of the development and design of fluidized bed reactors has been empirical in nature. This is due to the complex flow behaviour of gas-solid flow in these systems which makes flow modeling a challenging task.

The fundamental problem encountered in modeling hydrodynamics of fluidized bed is the motion of the two phases of which the interface is unknown and transient, and the interaction is understood only for a limited range of conditions [1].

Due to the mathematical complexities of the non-linearity of the equations and in defining the interpenetrating and moving phase boundaries numerical solutions are very difficult to achieve [2].

However, computational fluid dynamics (CFD) is emerging as a very promising new tool in modeling hydrodynamics. While it is now a standard tool for single-phase flows, it is at the development stage for multiphase systems, such as fluidized beds [3].

Many researchers have used commercial CFD codes for simulating multiphase problems and similar simulations were performed by Taghipour [4] in fluidized bed with the presence of air and sand using FLUENT 4.56. The research was carried out at various velocities. The performance of the code was better at higher gas velocities. Many researchers have simulated three-dimensional two fluids CFD model of gas particle flow in the CFB using the code CFX-4.3. The turbulence was modeled by k- ϵ turbulence model in the gas phase and a fixed particle viscosity model in the solid phase. This CFD model showed good agreement with the experiments [5]. A similar study of gas/particle flow behavior in the riser section of a circulating fluidized bed (CFB) was done using FLUENT 4.4. Fluid Catalytic Cracking (FCC) particles and air were used as the solid and gas phases, respectively. The computational results showed that the inlet and outlet design have significant effects on the overall gas and solid flow patterns and cluster formations in the riser [6].

CFB USED FOR SIMULATION

Figure 1 shows the schematics of the CFB used for simulation. This CFB is still in the commissioning phase and the experimentation work is expected to start soon. It consists of an air supply device (blower), a stainless steel distributor, a fast column of Plexiglas and primary and secondary cyclones of steel and a solid feeding system. The riser and its exit are made of Plexiglas to visualize the flow behaviour and to perform image analysis.

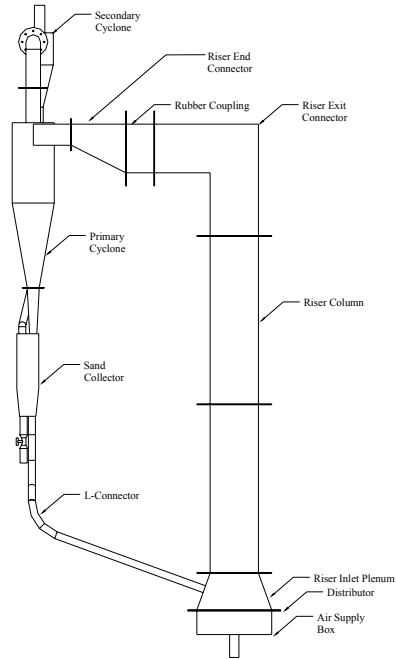


Figure 1 Circulating fluidized test rig at the Universiti Teknologi Malaysia

The 2D simulation work described here was done on a riser of rectangular cross-section of 265 mm (width) x 72 mm (depth) x 2649 mm (height). The 2D geometry was chosen to have an understanding of the flow profiles in riser with different exit geometries at little computational expense. The operating parameters were chosen as they used to appear in a large Circulating Fluidized Bed Combustors (CFBCs). Simulation was done using FLUENT a computational fluid dynamics (CFD) package produced and owned by Fluent Inc. [7]. Sand particles and air were used as the solid and gas phases, respectively. The parameters used in the simulation work are being summarized in Table 1.

Table 1 Parameters used in simulation work

Parameter	Range of values
Riser dimensions	2649 (L) X 265 (W) mm X 72 (D) mm
Gas velocity	5 m/s
Particle velocity	2 m/s
Properties of air	Density: 1.225 kg m ⁻³ Viscosity: 1.79 x 10 ⁻⁵ kg/m.s
Properties of particle (sand)	Density: 2500 kg m ⁻³ Diameter: 100X 10 ⁻⁶ m
Height of the sand inlet from distributor	200 mm
Exit Geometries Simulated	Right angle exit, right angle exit with baffle and blind T exit.
Volume fraction of sand	0.03 used as the Algebraic Slip Mixture Model gives good prediction within 10% volume fraction of sand
Granular properties	Particle-particle restitution coefficient is 0.95. Particle-wall restitution coefficient of 0.9
Multiphase model	Eulerian granular multiphase model

RISER EXIT

A wide range of experimental riser exits, which have been reported in the literature [8]. The bend exits shown are characterized by a centerline radius of curvature. Blind T exits are characterized by a roof extension height, a special case is the right angle exit, where extension height is zero. They are most commonly used in industrial CFBCs. These geometries are being shown in Figure 2.

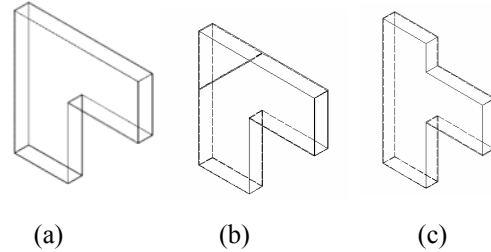


Figure 2 Riser Exits (a) Right angle exit (b) right angle exit with baffle (c) blind T exit

The findings of references [9] & [10] indicate that riser exits can affect the gross-behaviour of a CFB. If more solids accumulate near the riser exit then fewer solids reside in the return leg and therefore the static pressure head in the return leg are smaller. The lower rate of solids circulation may cause the solids volume fraction in the riser and connector to be lower. However, if the solids accumulation near the riser exit extends into these components, the solids volume fraction may be larger. The upstream exit region is generally characterized by a Core/Annulus (C/A) structure.

The four mechanisms which govern the solid motion in the riser exits are: inward/outward motion, secondary flow of the first kind, tangential acceleration/deceleration and cavity formation. These are being defined briefly below:

Inward /outward motion

Owing to their high density, solids in the core region of a riser exit may slip either to the outside or to the inside of the exit, dependent on the relative magnitudes of their inertia and the acceleration due to gravity g as shown in Figure 3. The ratio of solids inertia to gravity may be represented by the following Froude number (Fr_R):

$$Fr_R = \frac{\bar{u}_{st}^2}{g R} \quad (1)$$

Where

\bar{u}_{st} is cross section average solid velocity near the top of the riser

g is the acceleration due to gravity

R is the average radius of curvature of riser exit

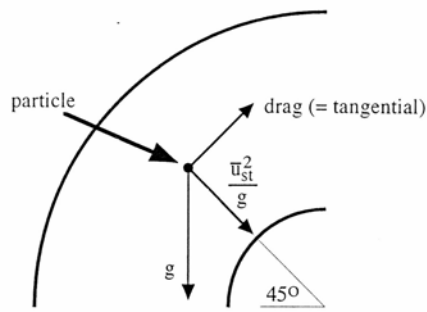


Figure 3 Motion of particle in exit bend (from, Meer [8])

The Froude number Fr_R is dependent on the cross-section average solids velocity near the top of the riser \bar{u}_{st} and on the average radius of curvature R , which is defined by:

$$R = \sqrt{R_{ei}^2 + R_{eo}^2} \quad (2)$$

Here R_{ei} and R_{eo} are the centerline radii of curvature at the inlet and outlet of the riser exit, respectively. The Froude number Fr_R may be expected to be a function of the exit geometry, the superficial gas velocity U_s and the superficial solids mass flow rate G_s .

Secondary flow of the first kind

Bends impose secondary flow of the first kind whereby high momentum fluid in the core moves to the outside of the bend, and slow moving fluid near the wall to the inside of the bend. As a result, the point of maximum velocity lies in the outer half of the bend. A high momentum suspension in the core of a riser exit may invoke similar lateral patterns. Figure 4 shows secondary flow patterns in a bend exit with a square cross-section.

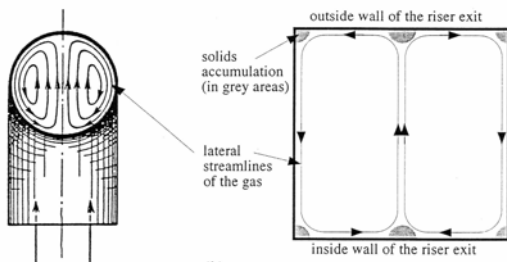


Figure 4 Secondary flow of first kind (from, Meer, [10])

It appears that velocity gradients are large near corners and in the middle of the inner and outer wall. Due to their high inertia, solids may accumulate in these areas.

Tangential acceleration /deceleration

Tangential acceleration or deceleration of the gas takes place in riser exits with cross-sections that change in size from inlet to outlet. A right angle exit with internal baffle yields acceleration followed by deceleration, a right angle or blind T exit yields deceleration followed by acceleration, and exits with unequal size inlet and outlet impose a net acceleration or deceleration.

Although solids may tend to retain their initial velocity due to their high inertia, they will slow down where the gas decelerates and speed up where the gas accelerates, due to drag between the phases. Since solids entrainment generally increases with the superficial gas velocity, a lower reflux is expected for regions of tangential acceleration and higher reflux for regions of tangential deceleration.

Cavity formation

Some riser exits may invoke cavities or regions where solids are disengaged from the main flow. An example is the blind T exit which invokes a cavity in the extension. Solids which enter the extension may hit the roof or, if the extension is sufficiently long, decelerate due to drag from the gas. Consequent build-up of downward momentum may enhance solids return to the riser. If all solids decelerate due to drag, any further extension of the roof may not increase the solids volume fraction in the riser and riser exit.

A small cavity or recirculation eddy may exist in the outer angle of the right angle exit, due to shear from two walls in this area. Cavities may also exist just below inlets of annular plate exits and below inlet baffles.

EULERIAN MULTIPHASE MIXTURE MODEL

The FLUENT modeling is based on the three-dimensional conservation equations for mass, momentum and energy. The differential equations are discretized by the Finite Volume Method and are solved by the SIMPLE algorithm. As a turbulence model, the $k-\epsilon$ was employed; this consists of two transport equations for the turbulent kinetic energy and its dissipation rate. The FLUENT code utilizes an unstructured non-uniform mesh, on which the conservation equations for mass, momentum and energy are discretized. The $k-\epsilon$ model describes the turbulent kinetic energy and its dissipation rate and thus compromises between resolution of turbulent quantities and computational time.

Table 2 List of FLUENT Models used in simulation

Model	Settings
Space	2D
Time	Steady
Viscous	Standard k-epsilon turbulence model
Wall Treatment	Standard Wall Functions
Multiphase Model	

In the FLUENT computer program that the governing equations were discretized using the finite volume technique. The discretized equations, along with the initial and boundary conditions, were solved to obtain a numerical solution.

The model used for simulating the gas-solid flow is the Eulerian Multiphase Mixture Model (EMMM). The EMMM solves the continuity equation for the mixture, the momentum equation for the mixture, and the volume fraction equation for the secondary phase, as well as an algebraic expression for the relative velocity.

By using the mixture theory approach, the volume of phase q , V_q is defined by

$$V_q = \int_V \alpha_q dV \quad (3)$$

$$\text{and} \quad \sum_{q=1}^n \alpha_q = 1 \quad (4)$$

$$\text{The effective density of phase } q \text{ is } \hat{\rho} = \alpha_q \rho_q \quad (5)$$

Where ρ_q is the physical density of phase .

3.1 Conservative Equations

The general conservation equations from which the solution is obtained by FLUENT are being presented below:

The continuity equation for phase q is

$$\frac{\partial}{\partial t} (\alpha_q \rho_q) + \nabla \cdot (\alpha_q \rho_q \vec{v}_q) = \sum_{p=1}^n \dot{m}_{pq} \quad (6)$$

where \vec{v}_q is the velocity of phase q and \dot{m}_{pq} characterizes the mass transfer from the pth to qth phase.

From the mass conservation we can get:

$$\dot{m}_{pq} = - \dot{m}_{qp} \quad (7)$$

$$\text{and} \quad \dot{m}_{pp} = 0 \quad (8)$$

Usually, the source term ($\sum_{p=1}^n \dot{m}_{pq}$) on the right hand side of the equation is zero.

The momentum balance for phase q yields

$$\begin{aligned} \frac{\partial}{\partial t} (\alpha_q \rho_q \vec{v}_q) + \nabla \cdot (\alpha_q \rho_q \vec{v}_q \vec{v}_q) = & -\alpha_q \nabla p + \\ \nabla \cdot \bar{\tau}_q + \alpha_q \rho_q \bar{g} + \sum_{p=1}^n (\bar{R}_{pq} + \dot{m}_{pq} \vec{v}_q) + & \\ \alpha_q \rho_q (\bar{F}_q + \bar{F}_{lift,q} + \bar{F}_{vm,q}) & \end{aligned} \quad (9)$$

Where $\bar{\tau}_q$ is the qth phase stress-strain tensor.

$$\bar{\tau}_q = \alpha_q \mu_q (\nabla \vec{v}_q + \nabla \vec{v}_q^T) + \alpha_q (\lambda_q - \frac{2}{3} \mu_q) \nabla \cdot \vec{v}_q \bar{I} \quad (10)$$

Here μ_q and λ_q are the shear and bulk viscosity of phase q, \bar{F}_q is an external body force, $\bar{F}_{lift,q}$ is a lift force, $\bar{F}_{vm,q}$ is a virtual mass force, \bar{R}_{pq} is an interaction force between phases, and p is the pressure shared by all phases.

\vec{v}_q is the interphase velocity and I can be defined as follows.

$$\text{If } \dot{m}_{pq} > 0 \text{ (i.e., phase p mass is being transferred to phase q),} \\ \vec{v}_{pq} = \vec{v}_p; \quad (11)$$

$$\text{If } \dot{m}_{pq} < 0 \text{ (i.e., phase q mass is being transferred to phase p),} \\ \vec{v}_{pq} = \vec{v}_q; \quad (12 a)$$

$$\vec{v}_{pq} = \vec{v}_{qp} \quad (12 b)$$

The above equation must be closed with appropriate expressions for the interphase force \bar{R}_{pq} . This force depends on the friction, pressure, cohesion, and other effects, and is subject to the conditions that

$$\bar{R}_{pq} = -\bar{R}_{qp} \text{ and } \bar{R}_{qq} = 0 \quad (13)$$

FLUENT uses the following form:

$$\sum_{p=1}^n \bar{R}_{pq} = \sum_{p=1}^n K_{pq} (\vec{v}_p - \vec{v}_q) \quad (14)$$

Where $K_{pq} = K_{qp}$ is the interphase momentum exchange coefficient.

TURBULENCE MODEL

In order to account for the effects of turbulent fluctuations of velocities the number of terms to be modeled in the momentum equations in multiphase is large and this makes the modeling of turbulence in multiphase simulations extremely complex. The turbulence model used for the current simulations is based on Mixture Turbulence Model (MTM). The κ and ε equations describing this model are as follows:

$$\frac{\partial}{\partial t} (\rho_m \kappa) + \nabla \cdot (\rho_m \vec{v}_m \kappa) = \nabla \cdot \left(\frac{\mu_{t,m}}{\sigma_\kappa} \nabla \kappa \right) + G_{\kappa,m} - \rho_m \varepsilon \quad (15)$$

$$\frac{\partial}{\partial t}(\rho_m \varepsilon) + \nabla \cdot (\rho_m \bar{v}_m \varepsilon) = \nabla \cdot \left(\frac{\mu_{t,m}}{\sigma_\varepsilon} \nabla \varepsilon \right) + \frac{\varepsilon}{\kappa} (C_{1\varepsilon} G_{\kappa,m} - C_{2\varepsilon} \rho_m \varepsilon) \quad (16)$$

Where the mixture density and velocity, ρ_m and \bar{v}_m , are computed from:

$$\rho_m = \sum_{i=1}^N \alpha_i \rho_i \quad (17)$$

$$\bar{v}_m = \frac{\sum_{i=1}^N \alpha_i \rho_i \bar{v}_i}{\sum_{i=1}^N \alpha_i \rho_i} \quad (18)$$

The turbulent viscosity, $\mu_{t,m}$, is computed from:

$$\mu_{t,m} = \rho_m C_\mu \frac{\kappa^2}{\varepsilon} \quad (19)$$

and the production of turbulence kinetic energy, $G_{\kappa,m}$, is computed from

$$G_{\kappa,m} = \mu_{t,m} (\nabla \bar{v}_m + (\nabla \bar{v}_m)^T) : \nabla \bar{v}_m \quad (20)$$

BOUNDARY CONDITIONS

At the inlet, all velocities and volume fractions of both phases are specified. The pressure is not specified at the inlet because of the incompressible gas phase assumption (relatively low pressure drop system). The initial velocity of gas and solid phase is being specified as mentioned in Table 1.

The meshing was done using Gambit 1.2. Fine meshing was done for riser inlet and exit sections in order to analyze them in a better way. Under relaxation factors were tuned to achieve convergence. The convergence tolerance was set at 0.001.

The main parameters of the flow inside the system are calculated using an iteration calculation procedure performed by FLUENT. An iterative cycle starts with the introduction of the initial data and/or initial guessed values, boundary conditions, physical conditions and constants. In a second step the program calculate the velocity field from the momentum equation. Then, the mass balance equations as well as the pressure equation are solved.

The next step is to update again the values of the parameters for both phases. The final step is to check on convergence which criterion is fixed by the user. If the convergence criterion is achieved the simulation will stop and give the final results of the system. If not, certain correction values are used to adjust the calculated values and the calculation will start all over again, using as initial data these last corrected values of each parameter.

The coefficient of restitution quantifies the elasticity of particle collisions. It has a value of 1 for fully elastic collisions and 0 for fully inelastic collisions. It is utilized to account for the loss of energy due to collision of particles, which is not considered in the classical kinetic theory. The restitution coefficient is close to unity. In this study, a particle-particle restitution coefficient of 0.95, and a particle-wall restitution coefficient of 0.9 were used.

RESULTS AND DISCUSSIONS

Riser exits can affect the gross behaviour of a CFB. If more solids accumulate near the riser exit then fewer solids reside in the return leg. The lower rate of solids circulation may cause the solids volume fraction in the riser and connector to be lower. However, if the solids accumulation near the riser exit extends into these components, the solids volume fraction may be larger.

Inward/outward motion, secondary flows of the first kind, tangential acceleration/deceleration, and cavity formation near riser exits is mechanisms can account for asymmetric flow in the exit region.

A right angle exit with internal baffle and a blind T riser exits show that the solids volume fraction is more or less constant in the lower half of the riser. In the upper half, a strong increase of solids volume fraction with elevation was observed for the blind T exit, whereas a decrease is found for the right angle exit with the internal baffle. This is illustrated in Figure 5.

The size and shape of the upstream exit region is strongly dependent on the design of the riser exit.

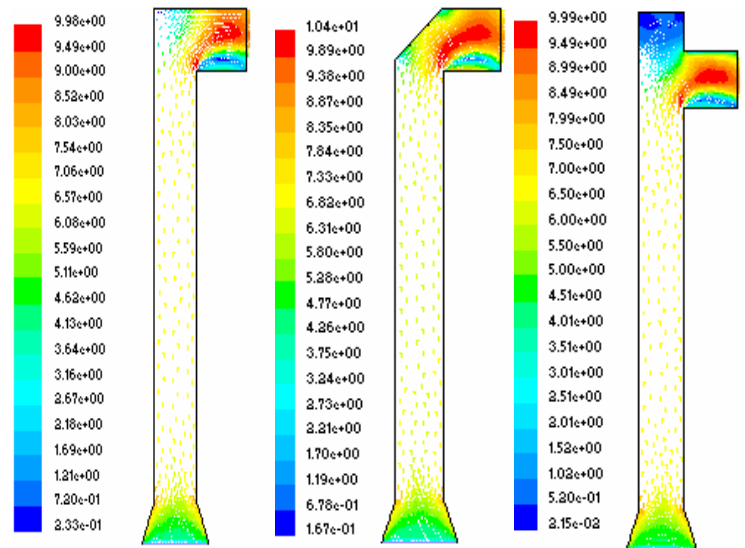


Figure 5 Contours of velocity profile in exit geometries

The right angle exit accumulated more solids than the long radius bend exit. The blind T exit accumulated more solids than the right angle exit, and yielded a higher solids volume fraction in the riser. The solids hold-up is greater for the exit with baffle. The blind T exit shows larger solids volume fractions along the entire riser height, and an increase of solids volume fraction with elevation in the upper half of the riser.

The solids volume fraction remains constant near the exit with internal baffle, but show an increase with elevation in the upper half of the riser for the right angle exit and blind T exit as shown in Figure 6.

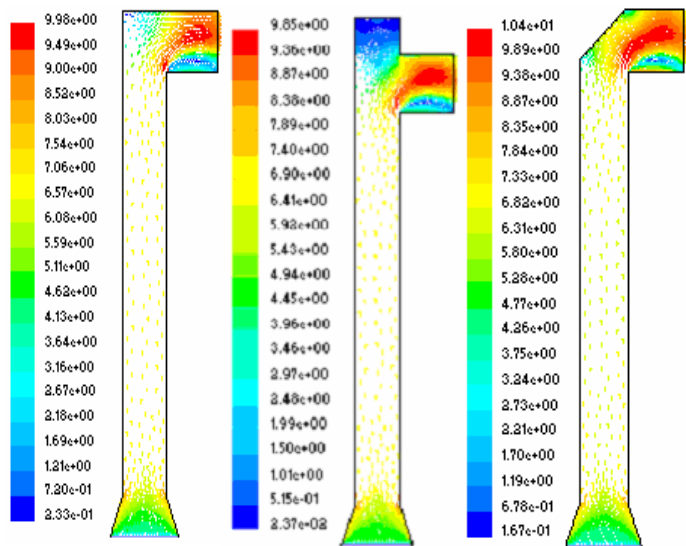


Figure 6 Contours of velocity by volume fraction of sand

The disengagement exit and the exit with internal baffle invoke an upstream exit region of reduced solids volume fraction. This bend exit yields little or no upstream exit region. The right angle exit, blind T exit and exits with inlet or outlet baffle cause an upstream exit region of increased solids volume fraction as shown in Figure 7. Larger blind T extension heights may invoke a greater upstream exit region, as long as they remain below a critical extension height. Medium size inlet or outlet baffles may yield greater upstream exit regions than large or small baffles.

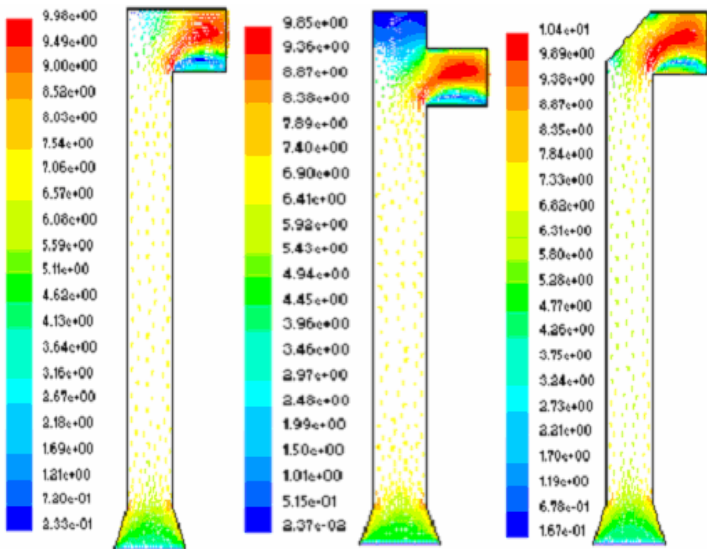


Figure 7 Contours of velocity by volume fraction of air

Figure 3. shows a particle in the middle of a bend exit, which experiences a radial acceleration (\bar{u}_{st}^2/R) equal to the radial component of the acceleration due to gravity ($g \cos 45^\circ$ or $g/\sqrt{2}$), i.e. $\bar{u}_{st}^2/R = g/\sqrt{2}$. This condition suggests that radial slip is minimized around $Fr_R = 1/\sqrt{2}$. Larger values of Fr_R may yield more movement of solids to the outside of the riser exit ('outward' movement), and smaller Froude numbers more movement to the inside of the riser exit ('inward' movement).

A radial acceleration balance suggests that inward/outward movement of solids in a riser exit is minimized around a Froude number $Fr_R = 1/\sqrt{2}$. Larger values of Fr_R yield more movement to the outside of the riser exit and smaller values more movement to the inside of the riser exit. From Figure 6 we can see that average exit velocity in the right angle exit bend is about 10 m/s which results in Fr_R much above the $1/\sqrt{2}$ value. So the predominant movement of the particles is outside of the riser exit. The same trend is also visible for other exits. However, the right angle exit with baffle show more pronounced movement outside the riser exit. It appears that Blind T has little effect of the extension height as compared to right angle exit. Figure 8 suggests that the slip is more prominent in the exit bends. The slip distribution are different with right angle exit and with baffle showing greater slip than blind T exit.

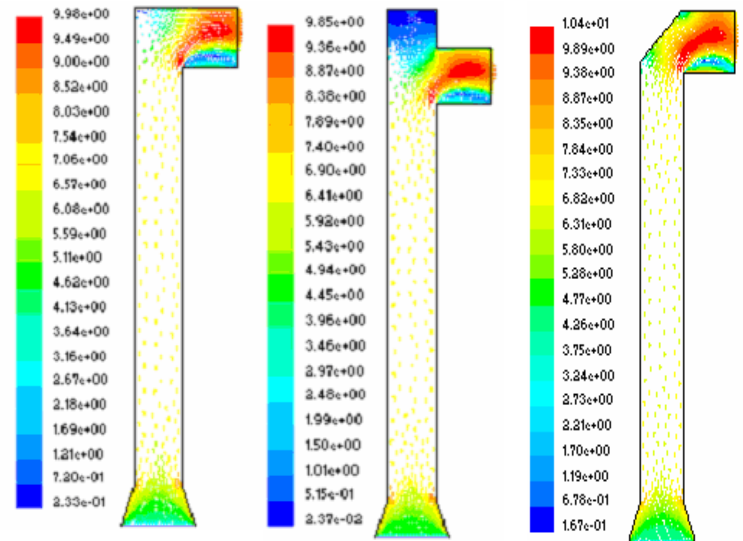


Figure 8 Contours of slip velocity

CONCLUSIONS

All the above investigations suggest that riser exits can reduce solids hold-up in the riser and yield a region upstream where the solids volume fraction decreases with elevation. Riser exits yield an apparently unaffected solids volume fraction profile or increased solids hold-up and invoke a region where the solids volume fraction increases with elevation.

This suggests an upstream exit region to be defined as the region upstream of the riser exit where flow properties are affected by the riser exit. Similarly, a downstream exit region can be defined as the region downstream of the riser exit where flow properties are affected by the riser exit. The (overall) exit region is the region of the CFB

where flow properties are affected by the riser exit, and comprises the upstream exit region, downstream exit region and the riser exit itself.

The results suggest that (i) the right angle exit and the right angle exit with internal baffle invoke an upstream exit region of reduced solids volume fraction, (ii) the bend exit yields little or no upstream exit region, and (iii) the right angle exit, blind T exit and exits with inlet or outlet baffle cause an downstream exit region of increased solids volume fraction.

The upstream exit region is generally characterized by a Core/Annulus structure, but that the solids mass flux profile may be asymmetric. Some riser exits appear to invoke regions near the riser wall where solids motion is upwards.

REFERENCES

- [1] Gilbertson, M.A. & Yates, J.G. (1996). The Motion of Particles Near a Bubble in a Gas-Fluidized Bed. *Journal of Fluid Mechanics* 323: 377-385
- [2] Pain, C.C., Mansoorzadeh, S. & de Oliveira, C.R.E. (2001). A Study of Bubbling and Slugging Fluidised Beds Using the Two-Fluid Granular Temperature Model. *International Journal of Multiphase Flow* 27, 527-551.
- [3] Taghipour, F., Ellis, N. & Clayton, W. (2003). CFD Modeling of a two-dimensional Fluidized Bed Reactor, University of British Columbia.
- [4] Jallil R., Tasirin S. & M. S. Takriff (2002). Computational Fluid Dynamics (CFD) in Fluidized Bed column: effect of Internal Baffles, The proceedings of RSCE Oct 2002, Malaysia.
- [5] Hansen, K. G., Madsen, J., Ibsen, C. H., Solberg T. & Hjertager B. H. (2002). An experimental and computational study of a gas-particle flow in a scaled circulating fluidized bed. *Presented at WCP74, World Congress on Particle Technology, 21-25 July, Sydney, NSW, Australia.*
- [6] Arastoopour, H., Benyahia, S., Knowlton, T. M. & Massah H. (2004) Simulation of particle and gas flow behavior in the riser section of a circulating fluidized bed using kinetic theory approach for the particulate phase. *Powder Technology (Articles in Press)*.
- [7] Fluent 6.1, (2001). User's guide. Fluent Incorporated.
- [8] Meer, E.H. (1997) Riser Exits and Scaling of Circulating Fluidised Beds, *Ph.D. theses*, University of Cambridge, UK.
- [9] Weinstein, H, H.J. Feindt, L. Chen, R.A. Graff (1992). The measurement of turbulence quantities in a high velocity fluidized bed. *Proceedings of 7th International Conference on Fluidization*, O.E. Potter, D.J. Nicklin (eds), Engineering Foundation, NY, 305 - 312.
- [10] Wu, S. & M. Alliston (1993). Cold model testing of the effects of air proportions and reactor outlet geometry on solids behaviour in a CFB, *Proceedings of 12th International Conference on Fluidized Bed Combustion*, L.N. Rubow, G. Commonwealth (Eds.), ASME, 1003 - 1009.